

# 行政院國家科學委員會專題研究計畫 成果報告

## 智能材料：磁致伸縮與壓電複合材料之電磁耦合效應 研究成果報告(精簡版)

計畫類別：個別型  
計畫編號：NSC 97-2218-E-009-041-  
執行期間：97年10月01日至98年07月31日  
執行單位：國立交通大學土木工程學系(所)

計畫主持人：郭心怡

計畫參與人員：碩士班研究生-兼任助理人員：馮俊憲

報告附件：出席國際會議研究心得報告及發表論文

處理方式：本計畫可公開查詢

中華民國 98 年 09 月 14 日

行政院國家科學委員會補助專題研究計畫  成果報告  
 期中進度報告

(計畫名稱)

智能材料：磁致伸縮與壓電複合材料之電磁耦合效應

計畫類別： 個別型計畫  整合型計畫

計畫編號：NSC 97-2218-E-009-041-

執行期間：2008年10月1日至2009年7月31日

計畫主持人：郭心怡

共同主持人：

計畫參與人員：馮俊憲

成果報告類型(依經費核定清單規定繳交)： 精簡報告  完整報告

本成果報告包括以下應繳交之附件：

赴國外出差或研習心得報告一份

赴大陸地區出差或研習心得報告一份

出席國際學術會議心得報告及發表之論文各一份

國際合作研究計畫國外研究報告書一份

處理方式：除產學合作研究計畫、提升產業技術及人才培育研究計畫、  
列管計畫及下列情形者外，得立即公開查詢

涉及專利或其他智慧財產權， 一年 二年後可公開查詢

執行單位：國立交通大學 土木工程學系

中華民國九十八年八月日

# Fibrous composites of piezoelectric and piezomagnetic phases

Hsin-Yi Kuo<sup>1\*</sup> and Kaushik Bhattacharya<sup>2</sup>

<sup>1</sup>Department of Civil Engineering,  
National Chiao Tung University,  
Hsinchu 30010, Taiwan

<sup>2</sup>Division of Engineering and Applied Science,  
California Institute of Technology, Pasadena, CA 91125, USA

## Abstract

We propose a theoretical framework for evaluation of magneto-electroelastic potentials in a fibrous composite with piezoelectric and piezomagnetic phases, motivated by the technological desire for materials with large magnetoelectric coupling. We show that the problem with transversely isotropic phases can be decomposed into two independent problems, plane strain with transverse electromagnetic fields and anti-plane shear with in-plane electromagnetic fields. We then consider the second problem in detail, and generalize the classic work of Lord Rayleigh [1] to obtain the electrostatic potential in an ordered conductive composite and its extension to a disordered system by Kuo and Chen [2] to the current coupled magneto-electroelastic problem. We use this method to study BaTiO<sub>3</sub>-CoFe<sub>2</sub>O<sub>4</sub> composites and provides insights into obtaining large effective magnetoelectric coefficient.

## 1 Introduction

A variety of technological applications including magnetic field sensors, magnetically controlled opto-electric devices and magneto-electric memories have motivated the study of magneto-electric coupling in materials and composites [3, 4]. The magneto-electric coupling was predicted by Landau and Lifshitz [5] and observed by Astrov [6] and by Rado and Folen [7] over fifty years ago. The coupling is weak in monolithic materials, and this has motivated the study of composites of piezoelectric and piezomagnetic media. The idea is that the applied magnetic field causes a deformation of the piezomagnetic material which in turn induces a deformation in the piezoelectric material thereby inducing an electric field.

The performance of a piezomagnetic/piezoelectric composite depends on the micro-geometry of the phases since one has to provide effective strain coupling and avoid electromagnetic

---

\*Corresponding author. E-mail: hykuo@mail.nctu.edu.tw

shielding. This has motivated a number of micromechanical models to predict the effective moduli of multiferroic composites. For example, Nan [8] and Huang and Kuo [9] used the Green’s function method to study a fibrous composite consisting of  $\text{BaTiO}_3$  and  $\text{CoFe}_2\text{O}_4$ . For such transversely isotropic fibrous composites, Benveniste [10] derived exact connections among effective magneto-electroelastic moduli using the uniform field concept. Particulate composites were investigated by Harshé *et al.* [11] using a cubic model and by Lee *et al.* [12] using finite element method. Eshelby’s approach and the mean field Mori-Tanaka model have been generalized to multiferroic composites by Li and Dunn [13, 14], Huang [15], Li [16], Wu and Huang [17], Huang and Zhou [18] and Srinivas *et al.* [19]. Frequency dependence of magnetoelectric coefficients of multiferroic laminates was studied by Bichurin *et al.* [20, 21]. Nan *et al.* [4] provide an extensive review of the literature and the state of the art.

However, much of this work uses approximate methods and models based on single inclusions, and focus on the effective properties of composites with somewhat uncontrolled microstructure. There is a need for exact methods that can be used to evaluate these approximate methods. Further, a method that provides the detailed fields is useful to provide insights for developing better microstructures and more complex processes like dielectric breakdown and failure [22]. Similarly, detailed statistical methods require the fields associated with multiple particles [23]. Furthermore, recent advances in synthesis allows the fabrication of composites with highly controlled microstructure. For example, Ren *et al.* [24] have recently used a diblock copolymer precursors to produce a self-assembled hexagonal array of CFO nanofibers in a PZT matrix. Therefore, there is a need for obtaining the fields and properties of composites with controlled microstructure. All of these motivate the current work.

In a classic work, Lord Rayleigh [1] computed the electric potential for a conducting composite consisting of a periodic array of inclusions (cylinders and spheres). This was extended to arbitrary arrangements by Kuo and Chen [2, 25]. These works concern single fields. In this paper, we generalize this methodology to multiple coupled fields, specifically electrostatic, magnetostatic and mechanical.

We consider a composite medium made of piezoelectric and piezomagnetic phases arranged in a microstructure consisting of parallel cylinders in a matrix in Section 2. We show in Section 2.1 that if the phases are transversely isotropic, then the general problem can be decomposed into two independent problems, plane strain with transverse electromagnetic fields and anti-plane shear with in-plane electromagnetic fields. We then focus on the latter problem for much of paper. We notice in Section 2.2 that the coupling between the fields occurs only through the interface conditions. We exploit this in Section 2.3 to obtain a representation of the solution. The basic idea is to follow Kuo and Chen [2] and expand each field in each medium in a series. We consider periodic arrays in Section 3. We obtain effective properties in Section 4, and significantly show that the macroscopic properties depend solely on a single expansion coefficient (amongst the infinite).

This methodology is illustrated in Section 5 using composites of  $\text{BaTiO}_3$  and  $\text{CoFe}_2\text{O}_4$ . We choose this material pair for its practical potential and also because it enables comparison with previous work. We observe that the composite medium has a nontrivial magnetoelectric coupling even though the individual components do not. Further, we observe significant difference between composites with BTO fibers in a CFO matrix and its complement.

We briefly comment on the first problem – the plane elasticity with transverse electro-

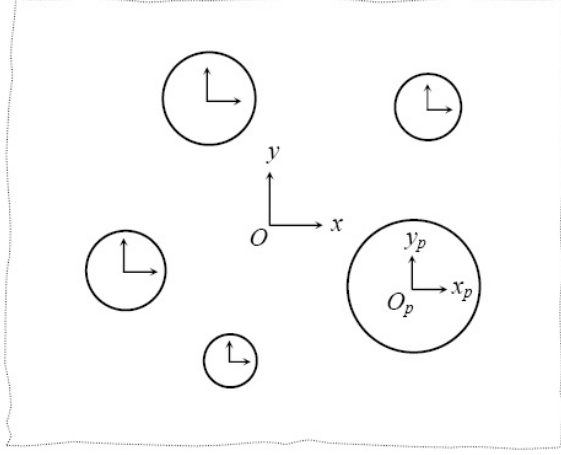


Figure 1: The cross-section of the fiber composite.

magnetic fields – in Section 6 and show the opportunity for extremely large magnetoelectric coupling.

## 2 Arbitrary arrangement of circular cylinders

### 2.1 General setting

Let us consider an infinite medium  $\mathbb{R}^3$  containing  $N$  arbitrarily distributed, parallel and separated circular cylinders. The domain of the  $p$ th circular cylinder is denoted  $V_p$ ,  $p = 1, 2, \dots, N$ , and the remaining matrix is denoted  $\Omega_m$ . We assume that the cylinders and the matrix are made of distinct phases<sup>1</sup>. Further, we assume that each phase is either piezoelectric or piezomagnetic. The constitutive laws for the  $r$ th phase is given by (see Alshits *et al.* [26], for example)

$$\begin{aligned}
 \sigma^{(r)} &= \mathbf{C}^{(r)} \varepsilon^{(r)} - \mathbf{e}^{T(r)} \mathbf{E}^{(r)} - \mathbf{q}^{T(r)} \mathbf{H}^{(r)}, \\
 \mathbf{D}^{(r)} &= \mathbf{e}^{(r)} \varepsilon^{(r)} + \kappa^{(r)} \mathbf{E}^{(r)} + \lambda^{(r)} \mathbf{H}^{(r)}, \\
 \mathbf{B}^{(r)} &= \mathbf{q}^{(r)} \varepsilon^{(r)} + \lambda^{(r)} \mathbf{E}^{(r)} + \mu^{(r)} \mathbf{H}^{(r)},
 \end{aligned} \tag{1}$$

where  $\sigma$ ,  $\mathbf{D}$ ,  $\mathbf{B}$ ,  $\varepsilon$ ,  $\mathbf{E}$  and  $\mathbf{H}$  are the stress, electric displacement, magnetic flux, strain, electric field, and the magnetic field respectively.  $\mathbf{C}$  is the fourth-order tensor of elastic moduli, and  $\kappa$ ,  $\mu$  and  $\lambda$  are the second order tensors of dielectric permittivity, magnetic permeability and magnetoelectric coefficients.

Now assume that each phase is transversely isotropic (i.e., has  $6mm$  symmetry) with the symmetry axes oriented with the cylinders. We introduce a Cartesian coordinate system with the  $x$ - and  $y$ - axes in the plane of the cross-section and  $z$ - along the axes of the cylinders. In the Voigt notation the properties  $\mathbf{C}$ ,  $\mathbf{e}$ ,  $\mathbf{q}$ ,  $\kappa$ ,  $\mu$ , and  $\lambda$  are given by Nye [27]:

<sup>1</sup>Later we shall specialize to a two-phase situation where all the cylinders belong to one phase and the matrix to another.

$$\begin{aligned}
\mathbf{C}^{(r)} &= \begin{pmatrix} C_{11} & C_{12} & C_{13} & 0 & 0 & 0 \\ C_{12} & C_{11} & C_{13} & 0 & 0 & 0 \\ C_{13} & C_{13} & C_{33} & 0 & 0 & 0 \\ 0 & 0 & 0 & C_{44} & 0 & 0 \\ 0 & 0 & 0 & 0 & C_{44} & 0 \\ 0 & 0 & 0 & 0 & 0 & C_{66} \end{pmatrix}^{(r)}, \\
\mathbf{e}^{(r)} &= \begin{pmatrix} 0 & 0 & 0 & 0 & e_{15} & 0 \\ 0 & 0 & 0 & e_{15} & 0 & 0 \\ e_{31} & e_{31} & e_{33} & 0 & 0 & 0 \end{pmatrix}^{(r)}, \\
\mathbf{q}^{(r)} &= \begin{pmatrix} 0 & 0 & 0 & 0 & q_{15} & 0 \\ 0 & 0 & 0 & q_{15} & 0 & 0 \\ q_{31} & q_{31} & q_{33} & 0 & 0 & 0 \end{pmatrix}^{(r)}, \\
\kappa^{(r)} &= \begin{pmatrix} \kappa_{11} & 0 & 0 \\ 0 & \kappa_{11} & 0 \\ 0 & 0 & \kappa_{33} \end{pmatrix}^{(r)}, \quad \mu^{(r)} = \begin{pmatrix} \mu_{11} & 0 & 0 \\ 0 & \mu_{11} & 0 \\ 0 & 0 & \mu_{33} \end{pmatrix}^{(r)}, \quad \lambda^{(r)} = \begin{pmatrix} \lambda_{11} & 0 & 0 \\ 0 & \lambda_{11} & 0 \\ 0 & 0 & \lambda_{33} \end{pmatrix}^{(r)}.
\end{aligned} \tag{2}$$

Consistent with known material properties, the magnetoelectric coupling coefficients  $\lambda^{(r)}$  is negligible though we do not explicitly use this fact here.

To obtain the effective properties of this medium, we need to solve for equilibrium equations

$$\nabla \cdot \boldsymbol{\sigma} = 0, \quad \nabla \cdot \mathbf{D} = 0, \quad \nabla \cdot \mathbf{B} = 0, \tag{3}$$

along with the analogous interfacial conditions and appropriate boundary conditions.

It is shown in the appendix, that for this cylindrical geometry and transversely isotropic material symmetry, the problem splits naturally into two *independent* problems:

- Plane strain and transverse electromagnetic fields

$$\mathbf{u} = \begin{pmatrix} u_x(x, y) \\ u_y(x, y) \\ 0 \end{pmatrix}, \quad \mathbf{E} = \begin{pmatrix} 0 \\ 0 \\ E_z(x, y) \end{pmatrix}, \quad \mathbf{H} = \begin{pmatrix} 0 \\ 0 \\ H_z(x, y) \end{pmatrix}, \tag{4}$$

- Anti-plane shear and in-plane electromagnetic fields

$$\mathbf{u} = \begin{pmatrix} 0 \\ 0 \\ u_z(x, y) \end{pmatrix}, \quad \mathbf{E} = \begin{pmatrix} E_x(x, y) \\ E_y(x, y) \\ 0 \end{pmatrix}, \quad \mathbf{H} = \begin{pmatrix} H_x(x, y) \\ H_y(x, y) \\ 0 \end{pmatrix}. \tag{5}$$

In other words, the solution to any general problem can be obtained by the superposition of the two problems above. Therefore, it is sufficient to treat each of these problems. In this work, we largely focus on the second, i.e., anti-plane shear with in-plane electromagnetic fields with brief comments on the first in Section 6.

## 2.2 Anti-plane shear with in-plane electromagnetic fields

We consider

$$\begin{aligned} u_x &= u_y = 0, \quad u_z = w(x, y), \\ \varphi &= \varphi(x, y), \\ \psi &= \psi(x, y), \end{aligned} \quad (6)$$

where  $u_x$ ,  $u_y$ ,  $u_z$  are the mechanical displacements along the  $x$ -,  $y$ -, and  $z$ - axes, and  $\varphi$  and  $\psi$  are the electric and magnetic potentials, respectively. The constitutive laws of the constituents and of the composite for the non-vanishing fields can be recast in the form

$$\begin{pmatrix} \sigma_{zj} \\ D_j \\ B_j \end{pmatrix} = \begin{pmatrix} C_{44} & e_{15} & q_{15} \\ e_{15} & -\kappa_{11} & -\lambda_{11} \\ q_{15} & -\lambda_{11} & -\mu_{11} \end{pmatrix} \begin{pmatrix} \varepsilon_{zj} \\ -E_j \\ -H_j \end{pmatrix} \quad (7)$$

where  $j$  denotes the component  $x, y$ . We can write this compactly as

$$\Sigma_{\Phi}^j = L_{\Phi\Psi} Z_{\Psi}^j, \quad \Phi, \Psi = w, \varphi, \psi, \quad j = x, y, \quad (8)$$

where

$$\Sigma^j = \begin{pmatrix} \sigma_{zj} \\ D_j \\ B_j \end{pmatrix}, \quad \mathbf{L} = \begin{pmatrix} C_{44} & e_{15} & q_{15} \\ e_{15} & -\kappa_{11} & -\lambda_{11} \\ q_{15} & -\lambda_{11} & -\mu_{11} \end{pmatrix}, \quad \mathbf{Z}^j = \begin{pmatrix} \varepsilon_{zj} \\ -E_j \\ -H_j \end{pmatrix}. \quad (9)$$

The shear strains  $\varepsilon_{zx}$  and  $\varepsilon_{zy}$ , in-plane electric fields  $E_x$  and  $E_y$ , and in-plane magnetic fields  $H_x$  and  $H_y$  can be derived from the gradient of elastic displacement, electric potential, and magnetic potential as follows:

$$\begin{aligned} \varepsilon_{zx} &= \frac{\partial w}{\partial x}, \quad \varepsilon_{zy} = \frac{\partial w}{\partial y}, \\ E_x &= -\frac{\partial \varphi}{\partial x}, \quad E_y = -\frac{\partial \varphi}{\partial y}, \\ H_x &= -\frac{\partial \psi}{\partial x}, \quad H_y = -\frac{\partial \psi}{\partial y}. \end{aligned} \quad (10)$$

In the absence of body force, electric charge density and electric current density, the equilibrium equations are given by

$$\begin{aligned} \frac{\partial \sigma_{zx}}{\partial x} + \frac{\partial \sigma_{zy}}{\partial y} &= 0, \\ \frac{\partial D_x}{\partial x} + \frac{\partial D_y}{\partial y} &= 0, \\ \frac{\partial B_x}{\partial x} + \frac{\partial B_y}{\partial y} &= 0. \end{aligned} \quad (11)$$

Substitution of Eq. (8) into Eq.(11) yields,

$$\begin{aligned} C_{44}\nabla^2 w + e_{15}\nabla^2\varphi + q_{15}\nabla^2\psi &= 0, \\ e_{15}\nabla^2 w - \kappa_{11}\nabla^2\varphi - \lambda_{11}\nabla^2\psi &= 0, \\ q_{15}\nabla^2 w - \lambda_{11}\nabla^2\varphi - \mu_{11}\nabla^2\psi &= 0, \end{aligned} \quad (12)$$

where  $\nabla^2 = \partial^2/\partial x^2 + \partial^2/\partial y^2$  represents the two-dimensional Laplace operator for the variables  $x$  and  $y$ . Since  $\mathbf{L}$  is a nonsingular matrix, generically we can decouple (12) into three independent Laplace equations,

$$\nabla^2 w = 0, \quad \nabla^2\varphi = 0, \quad \text{and} \quad \nabla^2\psi = 0 \quad (13)$$

in the interior of each phase. In other words, the three fields – displacement, electrostatic potential and magnetostatic potential – are completely decoupled in the interior of each phase.

In addition to these differential equations, we have to use interface and boundary conditions. We assume that the interfaces are perfectly bonded, and therefore the fields satisfy

$$[[\boldsymbol{\Sigma}^j \mathbf{n}^j]] = [[(\mathbf{L}\mathbf{Z}^j) \mathbf{n}^j]] = 0, \quad [[\mathbf{Z}^j \mathbf{t}^j]] = 0 \quad (14)$$

where  $[[\cdot]]$  denotes the jump in some quantity across the interface,  $\mathbf{n}$  is the unit normal to the interface and  $\mathbf{t}$  is the unit tangent to the interface, and the repeated index  $j$  denotes summing over the components  $x, y$ . Since  $\mathbf{L}$  is different in the two phases, the fields  $w, \varphi$  and  $\psi$  are generally coupled by the interface equations.

### 2.3 Representation of the solution

In the anti-plane shear problem, we showed above that the fields are decoupled in the interior of every phase, but are coupled at the interfaces. Therefore, we may follow Kuo and Chen [2] and use a series expansion for each field in the interior of each phase and then obtain the coefficients by enforcing the interface and boundary conditions.

We consider a situation where the composite is subjected to a macroscopically uniaxial loading

$$w_{\text{ext}} = \bar{\varepsilon}_{zx}x, \quad \varphi_{\text{ext}} = -\bar{E}_x x, \quad \psi_{\text{ext}} = -\bar{H}_x x, \quad (15)$$

for constants  $\bar{\varepsilon}_{zx}$ ,  $\bar{E}_x$  and  $\bar{H}_x$ . We may rewrite this in short as

$$\Phi_{\text{ext}} = \bar{Z}_{\Phi}^x x, \quad (16)$$

where  $\Phi$  represents the appropriate field – the anti-plane deformation  $w$ , electric potential  $\varphi$ , or magnetic potential  $\psi$  – and  $\bar{Z}_{\Phi}^x$  the corresponding applied field –  $\bar{\varepsilon}_{zx}$ ,  $-\bar{E}_x$ , or  $-\bar{H}_x$ .

We rewrite the governing equation, Eq. (13) in polar coordinates  $(r, \theta)$ ,

$$\nabla^2\Phi = \frac{\partial^2\Phi}{\partial r^2} + \frac{1}{r}\frac{\partial\Phi}{\partial r} + \frac{1}{r^2}\frac{\partial^2\Phi}{\partial\theta^2} = 0, \quad (17)$$

where  $\Phi$  can be  $w, \varphi$  or  $\psi$ . The potential field for the  $p$ th circular cylinder and its surrounding matrix can be expanded with respect to its center  $O_p$  as

$$\Phi_i^{(p)} = C_0^{\Phi^{(p)}} + \sum_{n=1}^{\infty} (C_n^{\Phi^{(p)}} r_p^n \cos n\theta_p + F_n^{\Phi^{(p)}} r_p^n \sin n\theta_p) \quad (18)$$



for the inclusion, and

$$\Phi_m^{(p)} = A_0^{\Phi(p)} + \sum_{n=1}^{\infty} [(A_n^{\Phi(p)} r_p^n + B_n^{\Phi(p)} r_p^{-n}) \cos n\theta_p + (D_n^{\Phi(p)} r_p^n + E_n^{\Phi(p)} r_p^{-n}) \sin n\theta_p] \quad (19)$$

for the matrix. Here  $(r_p, \theta_p)$  is the local polar coordinate centered at the origin of the  $p$ th circle, the subscripts  $i$  and  $m$  denote the inclusion and matrix, respectively. The coefficients  $A_n^{\Phi(p)}, B_n^{\Phi(p)}, \dots, F_n^{\Phi(p)}$  are some unknowns to be determined. The superscripts  $p$  in (18) and (19) indicate that the fields that are expanded with respect to the  $p$ th cylinder center.

We recall the interface conditions (14) which we rewrite as

$$\Phi_m^{(p)} \Big|_{\partial V_p} = \Phi_i^{(p)} \Big|_{\partial V_p}, \quad (\Sigma_{\Phi})_m^{(p)} \cdot \mathbf{n}_p \Big|_{\partial V_p} = (\Sigma_{\Phi})_i^{(p)} \cdot \mathbf{n}_p \Big|_{\partial V_p} \quad (20)$$

where

$$\Sigma_w = (\sigma_{zx}, \sigma_{zy}), \quad \Sigma_{\varphi} = (D_x, D_y), \quad \Sigma_{\psi} = (B_x, B_y), \quad (21)$$

$\partial V_p : r_p = a_p$  denotes the interface between the matrix and the  $p$ th circular cylinder, and  $\mathbf{n}_p$  is the unit outward normal of the interface  $\partial V_p$ .

Using the orthogonality properties of trigonometric functions, the conditions (20) provide

$$\mathbf{a}_n^{(p)} = a_p^{-2n} \mathbf{T}^{(p)} \mathbf{b}_n^{(p)}, \quad \mathbf{c}_n^{(p)} = a_p^{-2n} (\mathbf{T}^{(p)} + \mathbf{I}) \mathbf{b}_n^{(p)}, \quad (22)$$

$$\mathbf{d}_n^{(p)} = a_p^{-2n} \mathbf{T}^{(p)} \mathbf{e}_n^{(p)}, \quad \mathbf{f}_n^{(p)} = a_p^{-2n} (\mathbf{T}^{(p)} + \mathbf{I}) \mathbf{e}_n^{(p)}, \quad (23)$$

and  $A_0^{\Phi(p)} = C_0^{\Phi(p)}$ , where

$$\mathbf{a}_n^{(p)} = \begin{pmatrix} A_n^{w(p)} \\ A_n^{\varphi(p)} \\ A_n^{\psi(p)} \end{pmatrix}, \quad \mathbf{b}_n^{(p)} = \begin{pmatrix} B_n^{w(p)} \\ B_n^{\varphi(p)} \\ B_n^{\psi(p)} \end{pmatrix}, \quad \mathbf{c}_n^{(p)} = \begin{pmatrix} C_n^{w(p)} \\ C_n^{\varphi(p)} \\ C_n^{\psi(p)} \end{pmatrix}, \quad (24)$$

$$\mathbf{d}_n^{(p)} = \begin{pmatrix} D_n^{w(p)} \\ D_n^{\varphi(p)} \\ D_n^{\psi(p)} \end{pmatrix}, \quad \mathbf{e}_n^{(p)} = \begin{pmatrix} E_n^{w(p)} \\ E_n^{\varphi(p)} \\ E_n^{\psi(p)} \end{pmatrix}, \quad \mathbf{f}_n^{(p)} = \begin{pmatrix} F_n^{w(p)} \\ F_n^{\varphi(p)} \\ F_n^{\psi(p)} \end{pmatrix}, \quad (25)$$

$$\mathbf{T}^{(p)} = (\mathbf{L}^{(m)} - \mathbf{L}^{(p)})^{-1} (\mathbf{L}^{(m)} + \mathbf{L}^{(p)}), \quad (26)$$

and  $\mathbf{I}$  is the  $3 \times 3$  identity tensor.

We now need to relate the solutions to the applied boundary conditions. We do so by applying the Green's second identity [28] to the matrix domain  $\Omega_m$ . This gives

$$\begin{aligned} & \int_{\Omega_m} [G(\mathbf{x}; \mathbf{x}') \nabla'^2 \Phi_m(\mathbf{x}') - \Phi_m(\mathbf{x}') \nabla'^2 G(\mathbf{x}; \mathbf{x}')] dA' \\ &= \int_{\partial \Omega_m} [G(\mathbf{x}; \mathbf{x}') \nabla' \Phi_m(\mathbf{x}') - \Phi_m(\mathbf{x}') \nabla' G(\mathbf{x}; \mathbf{x}')] \cdot \mathbf{n}' ds', \end{aligned} \quad (27)$$

where the prime  $\prime$  denotes the operation in reference to the  $\mathbf{x}'$  coordinate,  $\mathbf{n}'$  is the outward unit normal to the matrix's boundary  $\partial \Omega_m$ ,  $dA'$  represents the area element for the  $\mathbf{x}'$

coordinate,  $ds'$  is the differential arc length. Here  $G(\mathbf{x}; \mathbf{x}')$  is the free-space Green's function for Laplace operator satisfying  $\nabla^2 G(\mathbf{x}; \mathbf{x}') = -\delta(\mathbf{x} - \mathbf{x}')$ , where  $\delta(\mathbf{x} - \mathbf{x}')$  is the Dirac-delta distribution. Following the procedure in Kuo and Chen [2], it can be shown that Eq. (27) yields

$$\Phi_m(\mathbf{x}) = \Phi_{\text{ext}}(\mathbf{x}) + \sum_{l=1}^N \sum_{m=1}^{\infty} (B_m^{\Phi(l)} r_l^{-m} \cos m\theta_l + E_m^{\Phi(l)} r_l^{-m} \sin m\theta_l). \quad (28)$$

This is the consistency equation which relates the external applied fields to the local potential expansions.

For convenience, we introduce the complex variable notation  $z = x + iy$  for  $\mathbf{x} = (x, y)$  with respect to the matrix and  $z_p$  for the cylinder centered at  $O_p$ . Now, equation (28) can be rewritten as

$$\Phi_m(\mathbf{x}) = \overline{Z}_{\Phi}^x z + \sum_{l=1}^N \sum_{m=1}^{\infty} [B_m^{\Phi(l)} \text{Re}(z - z_l)^{-m} - E_m^{\Phi(l)} \text{Im}(z - z_l)^{-m}], \quad (29)$$

where  $\overline{Z}_{\Phi}^x$  represents the corresponding applied field  $\overline{\varepsilon}_{zx}$ ,  $-\overline{E}_x$ , or  $-\overline{H}_x$ . Note that the field identity (29) is written based on different coordinates. To proceed, we shift the origin of the expansions (29) to a fixed point, say  $z_p$ . For point  $z$  satisfying the inequality  $|z - z_p| < |z_p - z_l|$ , we can then expand the term  $(z - z_l)^{-m}$  using the binomial theorem as [28]

$$(z - z_l)^{-m} = \sum_{s=0}^{\infty} (-1)^s \binom{m+s-1}{s} \frac{(z - z_p)^s}{(z_p - z_l)^{m+s}}. \quad (30)$$

Introducing (30) into (29), we have the expansion

$$\begin{aligned} \Phi_{m, \text{near}}^{(p)}(\mathbf{x}) &= \overline{Z}_{\Phi}^x \text{Re} z_p + \overline{Z}_{\Phi}^x \text{Re}(z - z_p) \\ &+ \sum_{m=1}^{\infty} [B_m^{\Phi(p)} \text{Re}(z - z_p)^{-m} - E_m^{\Phi(p)} \text{Im}(z - z_p)^{-m}] \\ &+ \sum_{l \neq p} \sum_{s=0}^{\infty} \sum_{m=1}^{\infty} (-1)^s \binom{m+s-1}{s} \\ &\times \left[ B_m^{\Phi(l)} \text{Re} \frac{(z - z_p)^s}{(z_p - z_l)^{m+s}} - E_m^{\Phi(l)} \text{Im} \frac{(z - z_p)^s}{(z_p - z_l)^{m+s}} \right] \end{aligned} \quad (31)$$

valid for the domain

$$|z - z_p| < \min(|z_p - z_l|), \text{ for } l = 1, 2, \dots, N, \text{ } p \neq l. \quad (32)$$

Since the expansion (31) are valid for points satisfying the condition (32), which generally applies to points near the  $p$ th inclusion, this expansion will be referred to as a near-field expansion, denoted as  $\Phi_{m, \text{near}}^{(p)}(\mathbf{x})$ . Further, since  $\mathbf{x}$  lies in the matrix domain, Equations

(31) and (19) should be identical. This provides the condition

$$\begin{aligned}
& A_0^{\Phi(p)} + \sum_{n=1}^{\infty} [A_n^{\Phi(p)} \operatorname{Re}(z - z_p)^n + D_n^{\Phi(p)} \operatorname{Im}(z - z_p)^n] \\
&= \overline{Z}_{\Phi}^x \operatorname{Re} z_p + \overline{Z}_{\Phi}^x \operatorname{Re}(z - z_p) + \sum_{l \neq p} \sum_{s=0}^{\infty} \sum_{m=1}^{\infty} (-1)^s \binom{m+s-1}{s} \times \\
&\quad \left[ B_m^{\Phi(l)} \operatorname{Re} \frac{(z - z_p)^s}{(z_p - z_l)^{m+s}} - E_m^{\Phi(l)} \operatorname{Im} \frac{(z - z_p)^s}{(z_p - z_l)^{m+s}} \right]. \tag{33}
\end{aligned}$$

Taking the real part and the imaginary part of (33), we find the two conditions

$$\begin{aligned}
& A_n^{\Phi(p)} - \sum_{l \neq p} \sum_{m=1}^{\infty} (-1)^n \binom{m+n-1}{n} [B_m^{\Phi(l)} \operatorname{Re}(z_p - z_l)^{-m-n} - E_m^{\Phi(l)} \operatorname{Im}(z_p - z_l)^{-m-n}] \\
&= \overline{Z}_{\Phi}^x \operatorname{Re} z_p \delta_{n,0} + \overline{Z}_{\Phi}^x \delta_{n,1}, \tag{34}
\end{aligned}$$

and

$$D_n^{\Phi(p)} + \sum_{l \neq p} \sum_{m=1}^{\infty} (-1)^n \binom{m+n-1}{n} [B_m^{\Phi(l)} \operatorname{Im}(z_p - z_l)^{-m-n} + E_m^{\Phi(l)} \operatorname{Re}(z_p - z_l)^{-m-n}] = 0. \tag{35}$$

Equations (34), (35), (22)<sub>1</sub>, and (23)<sub>1</sub> constitute an infinite set of linear algebraic equations. Upon appropriate truncations of the expansion terms, we can determine the expansion coefficients  $A_n^{\Phi(p)}$ ,  $B_n^{\Phi(p)}$ ,  $\dots$ ,  $F_n^{\Phi(p)}$ .

### 3 Periodic arrays

The analysis carried out in the previous section for the arbitrary system with a finite number of cylinders may also be adapted for the case of a periodic array of cylinders. There are five possible ways of packing cylinders in regular arrays in two dimensions (see [29], for instance). Here we concentrate on the two lattices, rectangular and hexagonal. Further, we sketch the outline of the derivation focussing on the differences from the previous situation. Finally, we limit ourselves to the case of anti-plane shear with in-plane electromagnetic fields.

Let us first introduce a Cartesian coordinate system  $(x, y)$  positioned at the center  $O$  of one of the cylinders in a square or a hexagonal array, as shown in Figure 2. The radius of the cylinders is  $a$  and we may assume unit distance between the centers of neighboring cylinders without loss of generality. Uniform intensities  $\overline{E}_x$  and  $\overline{H}_x$  are applied along the positive  $x$  axis, and an anti-plane shear deformation  $\overline{\varepsilon}_{zx}$  is applied out of the  $xy$  plane. In terms of polar coordinates, the general solution has the admissible form

$$\Phi_i = C_0^{\Phi} + \sum_{n=1}^{\infty} C_n^{\Phi} r^n \cos n\theta \tag{36}$$

for  $r < a$ , and

$$\Phi_m = A_0^{\Phi} + \sum_{n=1}^{\infty} (A_n^{\Phi} r^n + B_n^{\Phi} r^{-n}) \cos n\theta \tag{37}$$

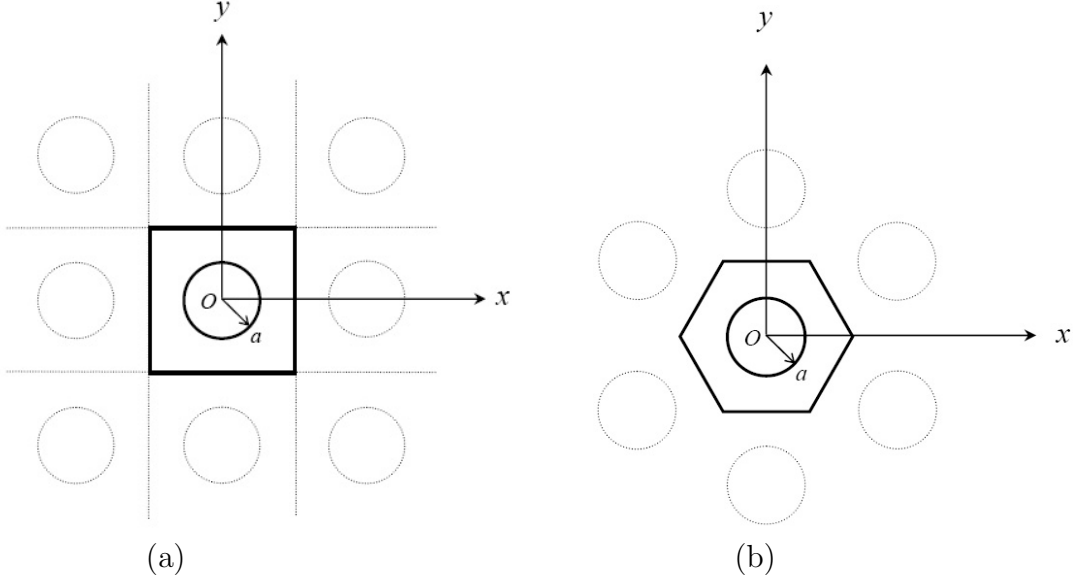


Figure 2: A schematic representation of a unit cell (a) A square array, (b) A hexagonal array.

for  $r > a$ . The coefficients  $A_n^\Phi$ ,  $B_n^\Phi$ , and  $C_n^\Phi$  are unknown constants to be determined from the interface and boundary conditions. Note that the sine terms that would be present in a general expansion are missing since we impose a uniaxial loading along the  $x$ - direction. Further,  $\Phi(r, \theta)$  has to be antisymmetric with respect to the  $y$ - axis, and thus only terms with an odd number are included. Finally, for a hexagonal lattice, all terms in which  $n$  is a multiple of three are disallowed [30].

Analogous to (22), the continuity conditions at the interface will give constraints (22) between the coefficients.

Next, imposing the periodicity conditions analogous to imposing the boundary condition we did to derive (34), leads to a generalized Rayleigh's identity

$$A_n^\Phi + \sum_{m=1}^{\infty} \binom{m+n-1}{n} S_{m+n} B_m^\Phi = \bar{Z}_\Phi^x \delta_{n,1}. \quad (38)$$

Here the quantities

$$S_m = \sum_{l \neq o} \text{Re} z_l^{-m} \quad (39)$$

are the lattice sums characterizing the geometry of the periodic structure, and  $z_l$  is the center of the  $l$ th cylinder when measured at the central point  $O$ . The index  $l$  runs over all cylinders' centers underlying the periodic array except the central one. A list of non-zero normalized lattice sums for square and hexagonal arrays can be found in Berman and Greengard [31].

Equations (38) and (22)<sub>1</sub> constitute an infinite set of linear algebraic equations. Upon appropriate truncations of the expansion terms, we can determine the expansion coefficients  $A_n^\Phi$ ,  $B_n^\Phi$ , and  $C_n^\Phi$ .

## 4 Effective moduli

We are interested in the effective behavior for a situation where we have a large number of cylinders. The effective material properties are defined in terms averaged fields,

$$\langle \boldsymbol{\Sigma}^j \rangle \equiv \mathbf{L}^* \langle \mathbf{Z}^j \rangle, \quad (40)$$

where the angular brackets denote the average over the representative volume element (unit cell in the case of periodic composites)

$$\langle \boldsymbol{\Sigma}^j \rangle = \frac{1}{V} \int_V \boldsymbol{\Sigma}^j d\mathbf{x}, \quad \langle \mathbf{Z}^j \rangle = \frac{1}{V} \int_V \mathbf{Z}^j d\mathbf{x}, \quad (41)$$

and  $\mathbf{L}^*$  denotes the effective magneto-electroelastic parameters of the composite.

We can compute the average  $\mathbf{Z}^j$  by noting that each component is a gradient and applying the divergence theorem. We obtain

$$\langle Z_{\Phi}^x \rangle = \overline{Z_{\Phi}^x}. \quad (42)$$

Next, to find  $\langle \Sigma_{\Phi}^x \rangle$ , we again use the divergence theorem and the equilibrium condition (including the interface conditions) to obtain:

$$\langle \Sigma_{\Phi}^x \rangle = \frac{1}{V} \int_V \Sigma_{\Phi}^x d\mathbf{x} = \frac{1}{V} \int_V \nabla \cdot (x \boldsymbol{\Sigma}_{\Phi}) d\mathbf{x} = \frac{1}{V} \int_{\partial V} x (\boldsymbol{\Sigma}_{\Phi})_m \cdot \mathbf{n} ds, \quad (43)$$

where  $\boldsymbol{\Sigma}_{\Phi}$  is defined in (21). We then use the expansions (19) for the fields to obtain

$$\frac{1}{V} \int_{\partial V} x (\mathbf{Z}_{\Phi})_m \cdot \mathbf{n} ds = \overline{Z_{\Phi}^x} - 2 \sum_{l=1}^N a_l^{-2} f_l B_1^{\Phi(l)}, \quad (44)$$

where

$$\mathbf{Z}_w = (\varepsilon_{zx}, \varepsilon_{zy}), \quad \mathbf{Z}_{\varphi} = -(E_x, E_y), \quad \mathbf{Z}_{\psi} = -(H_x, H_y), \quad (45)$$

and  $f_l$  is the volume fraction of phase  $l$  defined as  $f_l = \pi a_l^2/V$  for square arrays and is  $\frac{2\pi}{\sqrt{3}} a_l^2/V$  for hexagonal arrays. Putting (43) and (44) together, and recalling the constitutive relation (7) for the matrix, we obtain

$$\begin{pmatrix} \langle \sigma_{zx} \rangle \\ \langle D_x \rangle \\ \langle B_x \rangle \end{pmatrix} = \begin{pmatrix} C_{44} & e_{15} & q_{15} \\ e_{15} & -\kappa_{11} & -\lambda_{11} \\ q_{15} & -\lambda_{11} & -\mu_{11} \end{pmatrix}^{(m)} \begin{pmatrix} \overline{\varepsilon}_{zx} - 2 \sum_{l=1}^N a_l^{-2} f_l B_1^{w(l)} \\ -\overline{E}_x - 2 \sum_{l=1}^N a_l^{-2} f_l B_1^{\varphi(l)} \\ -\overline{H}_x - 2 \sum_{l=1}^N a_l^{-2} f_l B_1^{\psi(l)} \end{pmatrix}. \quad (46)$$

Putting together (40) and (46) and noting that the coefficients  $B_1^{\Phi}$  depend linearly on the applied field  $\overline{Z_{\Phi}^x}$ , we obtain set of equations for the effective property  $\mathbf{L}^*$ . We can determine this by applying different loading combinations between  $\overline{\varepsilon}_{zx}$ ,  $\overline{E}_x$  and  $\overline{H}_x$ .

Table 1: Material parameters of BaTiO<sub>3</sub> and CoFe<sub>2</sub>O<sub>4</sub> [14]

Property	BaTiO <sub>3</sub>	CoFe <sub>2</sub> O <sub>4</sub>
$C_{44}$ (N/m <sup>2</sup> )	$43 \times 10^9$	$45.3 \times 10^9$
$e_{15}$ (C/m <sup>2</sup> )	11.6	0
$q_{15}$ (N/Am)	0	550
$\kappa_{11}$ (C <sup>2</sup> /Nm <sup>2</sup> )	$11.2 \times 10^{-9}$	$0.08 \times 10^{-9}$
$\mu_{11}$ (Ns <sup>2</sup> /C <sup>2</sup> )	$5 \times 10^{-6}$	$-590 \times 10^{-6}$
$\lambda_{11}$ (Ns/VC)	0	0

## 5 Numerical results and discussion

In order to have a better understanding for the theoretical results above, we perform a numerical computation for a two-phase transversely isotropic piezoelectric-piezomagnetic composite with  $6mm$  material symmetry about the fiber axis. Specifically we consider a composite of BaTiO<sub>3</sub> and CoFe<sub>2</sub>O<sub>4</sub> which has been studied by other researchers. We consider square and hexagonal arrays, and both case, i.e., both BTO fibers in a CFO matrix and CFO fibers in a BTO matrix. The independent material constants of these constituents are given in Table I, where the  $xy$  plane is isotropic and the unique axis is along the  $z$ - direction. Note that in both materials magnetoelectric coefficients are zero, i.e.  $\lambda_{11} = 0$ .

We begin with a composite of BTO fibers in a CFO matrix. Figure 3 shows the effective elastic, dielectric, magnetic, piezoelectric, piezomagnetic and magnetoelectric moduli for this composite. They vary nonlinearly with volume fraction, and the curves stop at  $f = \pi/4$  and  $f = \pi/2\sqrt{3}$  for the square and hexagonal arrays respectively, when the inclusions touch. The magnetoelectric coefficient is non-zero for every (non-zero) volume fraction even though this coefficient is zero for each component. This reflects the coupling of the various fields across the boundary. Further, it initially increases with increasing volume fraction, then reaches a maximum before dropping just as the fibers are close to touching. To gain insight into this behavior, we plot the contours of displacement, electric potential and magnetic potential for a square array in Figure 5(a-c) with an applied magnetic field. The magnetic field induces a mechanical stress in the CFO which in turn results in an electric displacement in the BTO fiber. The effective electric displacement in the horizontal direction depends on the average along the vertical direction. Thus, the effective electric displacement depends on the span of the fiber in the vertical direction. This is why the ME coefficient starts at zero and increases with volume fraction. The magnetic field is attracted by the BTO (since it has a smaller magnetic permeability) and thus the scaling deviates from being proportional to the span and is close to linear initially. Further, as the particles come close to touching, there is very little CFO to induce stress and thus the ME coefficient drops dramatically.

Finally, Figure 3 also compares the effective moduli with those predicted by Benveniste [10] who used the composite cylinder assemblage (CCA) which is a mean-field theory. In CCA, there is no upper limit on the volume fraction since one can have fibers with various sizes. Still, the overall magnitudes and trends agree well between our periodic and his CCA.

We now turn to the composite of CFO fibers in a BTO matrix. Figure 4 shows the effective moduli for this composite. Again, magnetoelectric coefficient is non-zero for every

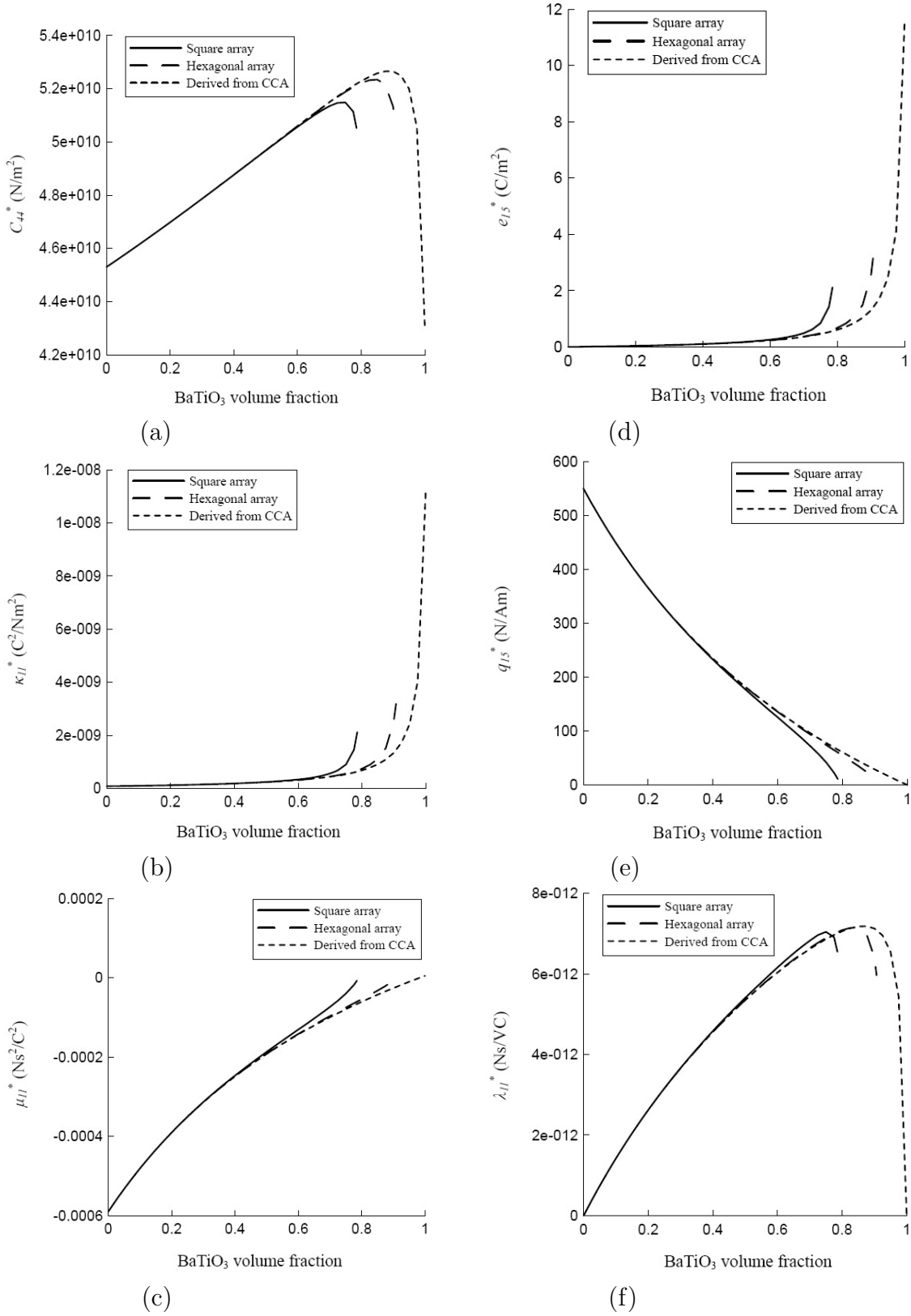


Figure 3: Effective moduli of a composite of BTO fibers in a CFO matrix versus BTO fiber volume fractions (a) Effective elastic modulus, (b) Effective dielectric permittivity, (c) Effective magnetic permeability, (d) Effective piezoelectric modulus, (e) Effective piezomagnetic modulus, (f) Effective magnetoelastic coefficient.

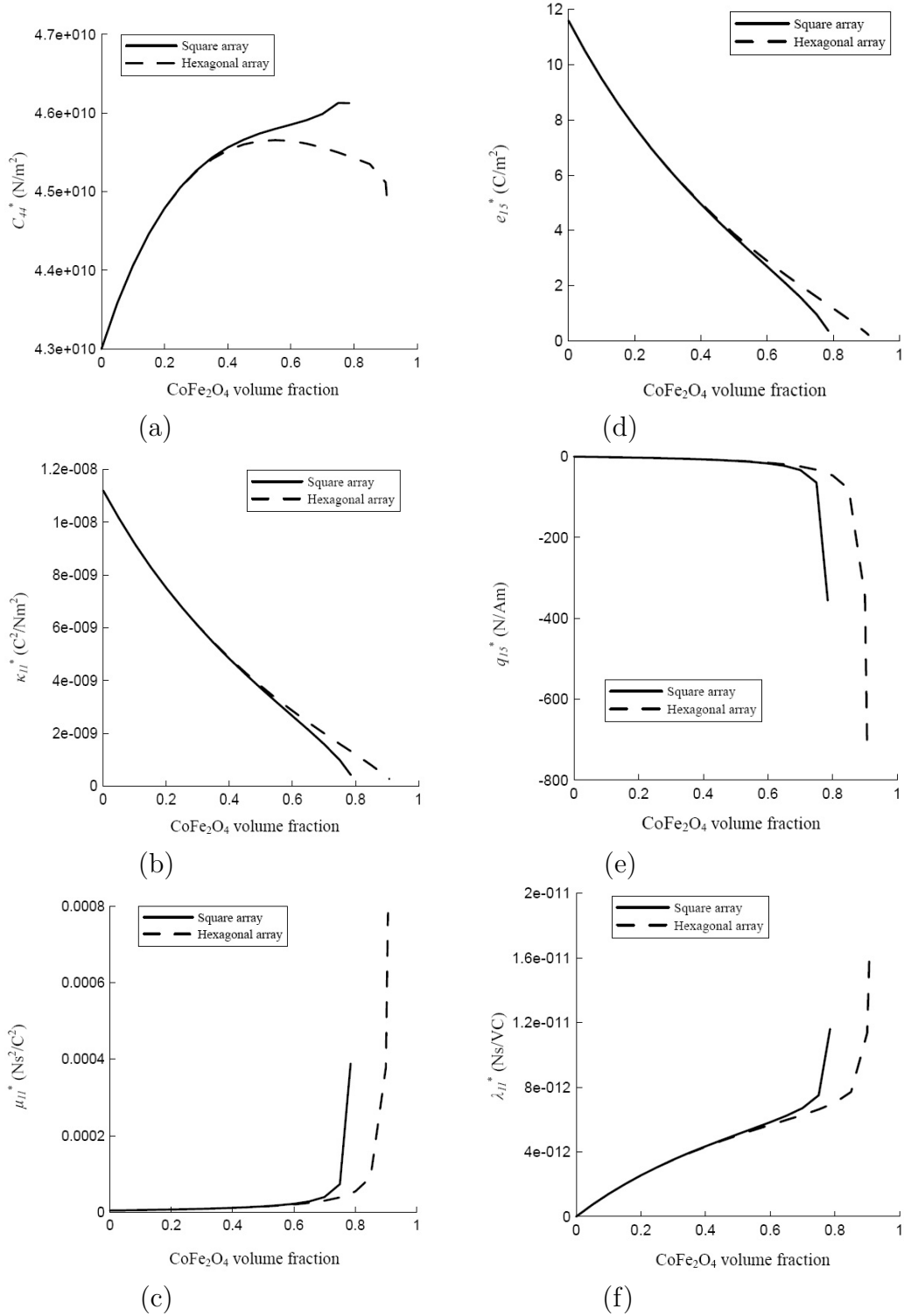


Figure 4: Effective moduli of a composite of CFO fibers in a BTO matrix versus CFO fiber volume fractions (a) Effective elastic modulus, (b) Effective dielectric permittivity, (c) Effective magnetic permeability, (d) Effective piezoelectric modulus, (e) Effective piezomagnetic modulus, (f) Effective magnetoelastic coefficient.



(non-zero) volume fraction even though this coefficient is zero for each component. However, in this case it is monotone increasing with a sharp rise as the particles are close to touching. Figure 5(d-f) show the potential contours for an applied magnetic field. Now, the magnetic field is expelled by the fibers giving rise to a displacement which deforms the matrix to induce an electric displacement. The amount of deformation it can cause in the matrix increases with volume fraction, and this is reflected in the magnetoelectric coefficient. Further, it increases dramatically as the particles touch.

We finally turn to the magnetoelectric voltage coefficient, which is the important figure of merit for magnetic field sensors. It relates the overall electric field that is generated in the composite when it is subjected to a magnetic field. It combines the coupling and dielectric coefficients, and is defined by

$$\alpha_{E11}^* = \lambda_{11}^*/\kappa_{11}^*. \quad (47)$$

Figure 6 shows how this coefficient depends on the volume fraction for the various cases. Note that there is a qualitative difference between the case of BTO fibers in CFO and its complement. In the former, the maximum coefficient is for an intermediate volume fraction of  $f = 0.35$  where  $\alpha_{E11}^* = 0.0306 \text{ V/cmOe}$  independent of the square or hexagonal geometry. In contrast, in the case of CFO fibers in the BTO matrix, the maximum is attained as the fibers begin to touch. These trends are similar to those of the magnetoelectric coefficient described before, and follow from the same reasons.

## 6 Plane strain with transverse electromagnetic fields

We briefly discuss the other problem described in (4), and the potential for using it for large effective magnetoelectric coefficient. Consider a situation where the average normal stress as well as the average electric displacement along the fibers are zero

$$\langle \sigma_{zz} \rangle = 0, \quad \langle D_z \rangle = 0. \quad (48)$$

The constitutive equations (2) specialized to the current setting (see (A.1) and (A.2)) then implies that

$$\langle C_{33} \rangle \varepsilon_{zz} = -\langle C_{13} (\varepsilon_{xx} + \varepsilon_{yy}) \rangle + \langle e_{33} \rangle E_z + \langle q_{33} \rangle H_z, \quad (49)$$

$$\langle e_{33} \rangle \varepsilon_{zz} = -\langle e_{31} (\varepsilon_{xx} + \varepsilon_{yy}) \rangle - \langle \kappa_{33} \rangle E_z - \langle \lambda_{33} \rangle H_z. \quad (50)$$

Eliminating  $\varepsilon_{zz}$  between the two equations above, we obtain

$$\frac{\langle e_{33} \rangle}{\langle C_{33} \rangle} (-\langle C_{13} (\varepsilon_{xx} + \varepsilon_{yy}) \rangle + \langle e_{33} \rangle E_z + \langle q_{33} \rangle H_z) = -\langle e_{31} (\varepsilon_{xx} + \varepsilon_{yy}) \rangle - \langle \kappa_{33} \rangle E_z - \langle \lambda_{33} \rangle H_z, \quad (51)$$

or

$$\begin{aligned} \left( \frac{\langle e_{33} \rangle^2}{\langle C_{33} \rangle} + \langle \kappa_{33} \rangle \right) E_z &= \frac{\langle e_{33} \rangle \langle C_{13} (\varepsilon_{xx} + \varepsilon_{yy}) \rangle}{\langle C_{33} \rangle} - \langle e_{31} (\varepsilon_{xx} + \varepsilon_{yy}) \rangle \\ &\quad - \left( \frac{\langle e_{33} \rangle \langle q_{33} \rangle}{\langle C_{33} \rangle} + \langle \lambda_{33} \rangle \right) H_z. \end{aligned} \quad (52)$$

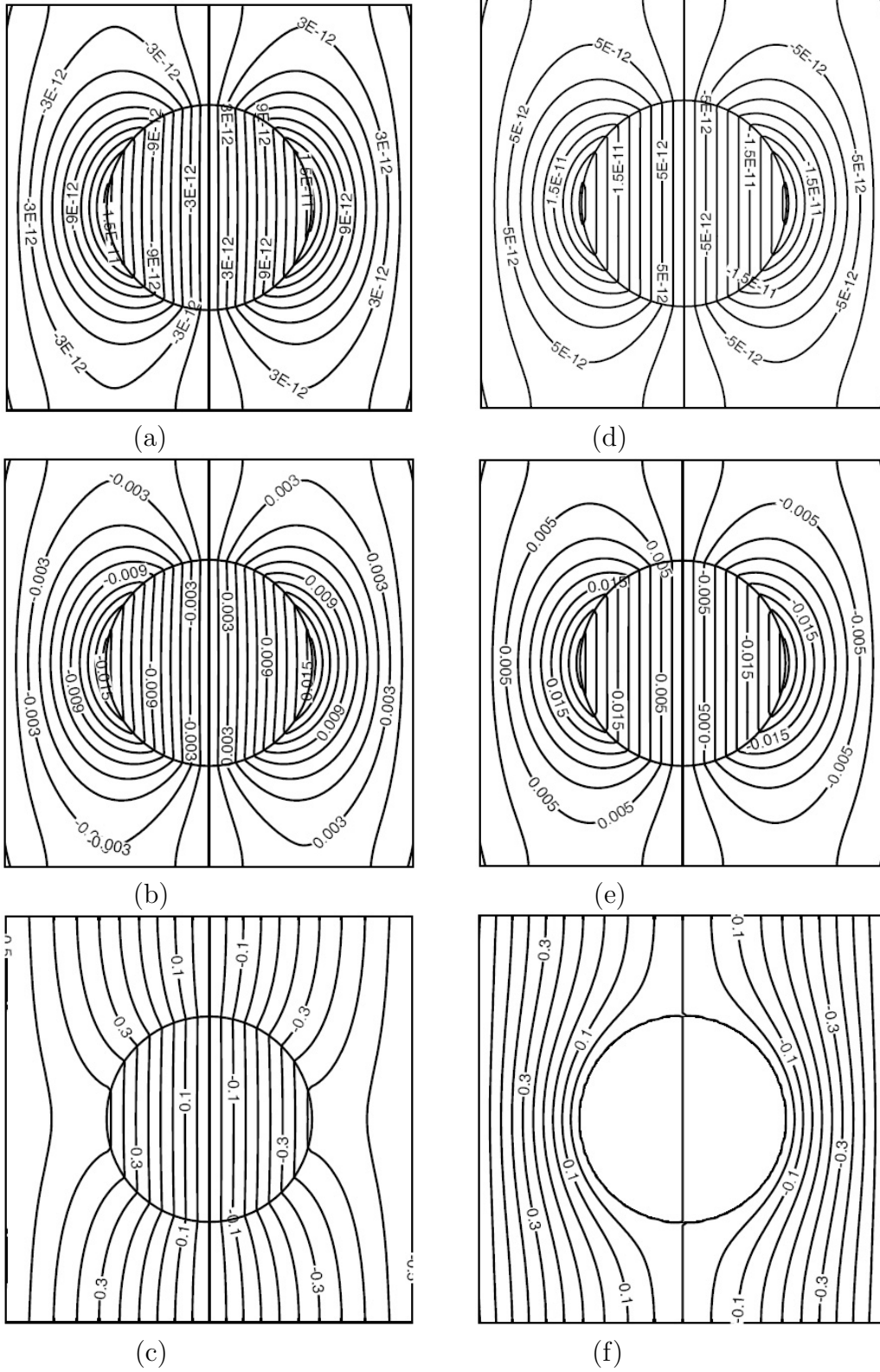


Figure 5: Potential contours for a square array composite ( $f = 0.2, \bar{\varepsilon}_{zx} = 0, \bar{E}_x = 0, \bar{H}_x = 1C/ms$ ) (a)-(c) BTO fibers embedded in a CFO matrix, (d)-(f) CFO fibers embedded in a BTO matrix, (a), (d) Vertical displacement ( $m$ ), (b), (e) Electric potential ( $V$ ), (c), (f) Magnetic potential ( $C/s$ ).

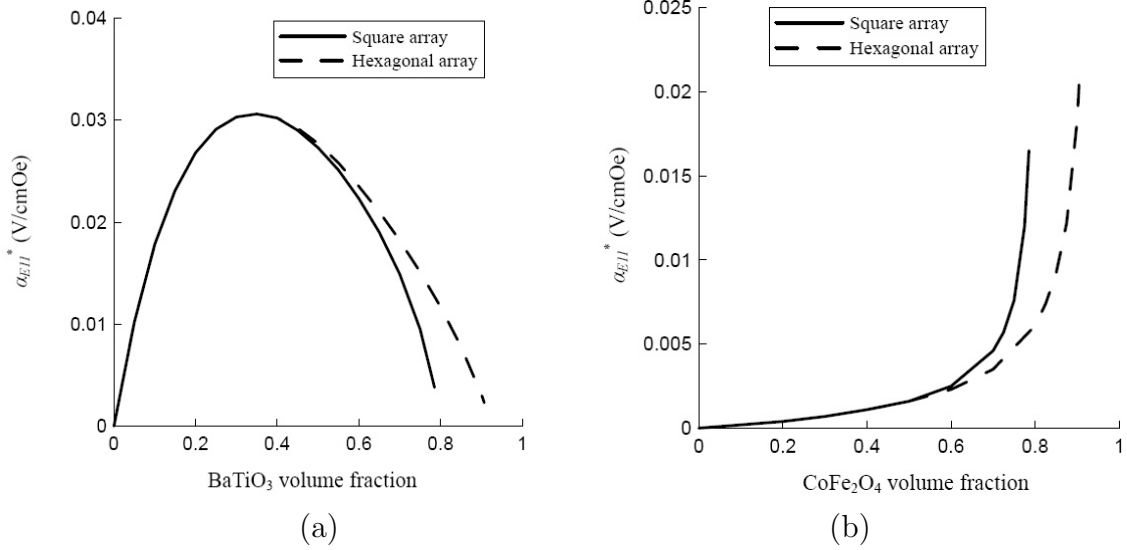


Figure 6: Effective magnetolectric voltage coefficient of the composite versus the fiber volume fraction. (a) BTO fibers in a CFO matrix. (b) CFO fibers in a BTO matrix.

We now assume further that the average planar strain is zero (alternately, we can proceed exactly the same if the effective planar stress is zero). Then, strain depends linearly on  $E_z$  and  $H_z$ , and thus, we can write

$$\frac{\langle e_{33} \rangle \langle C_{13} (\varepsilon_{xx} + \varepsilon_{yy}) \rangle}{\langle C_{33} \rangle} - \langle e_{31} (\varepsilon_{xx} + \varepsilon_{yy}) \rangle = AE_z + BH_z. \quad (53)$$

$A$  and  $B$  depend on the solution of the plane strain homogenization problem. Substituting (53) into (52), we obtain

$$\left( \frac{\langle e_{33} \rangle^2}{\langle C_{33} \rangle} - A + \langle \kappa_{33} \rangle \right) E_z = \left( B - \frac{\langle e_{33} \rangle \langle q_{33} \rangle}{\langle C_{33} \rangle} - \langle \lambda_{33} \rangle \right) H_z. \quad (54)$$

The magnetolectric voltage coefficient is the ratio of the two terms in parenthesis,

$$\alpha_{E_{33}}^* = \frac{B - \frac{\langle e_{33} \rangle \langle q_{33} \rangle}{\langle C_{33} \rangle} - \langle \lambda_{33} \rangle}{\frac{\langle e_{33} \rangle^2}{\langle C_{33} \rangle} - A + \langle \kappa_{33} \rangle}. \quad (55)$$

In particular, we concentrate on the denominator. Notice that only  $A$  depends on the microgeometry and the planar moduli where as the rest of the terms do not. Thus, it is possible to tune the microgeometry to reduce the denominator to get extremely large coupling.

We may use the methodology described in this paper to compute  $A$  and  $B$ . However, in contrast to anti-plane shear, plane strain elasticity is a vectorial problem and thus the method is significantly more difficult to implement. This is the topic of current work and will be presented elsewhere.

## 7 Concluding remarks

In summary, we have extended Rayleigh's formulation on periodic conductive composites to a magneto-electroelastic composite consisting of arbitrarily distributed or periodic arrays of cylinders under anti-plane shear deformation, in-plane electric and in-plane magnetic intensities. Expressions for the elastic, electric and magnetic potentials for the cylinders and the matrix are derived, and used to compute the effective moduli. It is shown that the effective properties solely depend on one particular constant  $B_1^\Phi$  among the infinite number of expansion coefficients. Finally, as a practical example, explicit numerical calculations for field distributions and the magnetoelectric effects in BaTiO<sub>3</sub>-CoFe<sub>2</sub>O<sub>4</sub> composites are presented and discussed. This example shows the important difference between the case of BTO fibers in a CFO matrix from its complement. The present theoretical framework provides a general guideline for the selection of the best combination with an efficient coupling of piezoelectric and piezomagnetic properties. It can also provide a rigorous basis against which several approximate micromechanical models can be compared.

## Acknowledgment

H.-Y. Kuo is grateful to National Science Council, Taiwan, under contract NSC-0-97-2218-E-009-041. We are also grateful to the financial support of the US Army Research Office (W911NF-07-1-0410).

## Appendix

We substitute Eq. (2) into Eq.(1) and obtain

$$\begin{bmatrix} \sigma_{xx} \\ \sigma_{yy} \\ \sigma_{zz} \\ \sigma_{zy} \\ \sigma_{zx} \\ \sigma_{xy} \end{bmatrix} = \begin{bmatrix} C_{11}\varepsilon_{xx} + C_{12}\varepsilon_{yy} + C_{13}\varepsilon_{zz} \\ C_{12}\varepsilon_{xx} + C_{11}\varepsilon_{yy} + C_{13}\varepsilon_{zz} \\ C_{13}\varepsilon_{xx} + C_{13}\varepsilon_{yy} + C_{33}\varepsilon_{zz} \\ 2C_{44}\varepsilon_{zy} \\ 2C_{44}\varepsilon_{zx} \\ 2C_{66}\varepsilon_{xy} \end{bmatrix} - \begin{bmatrix} e_{31}E_z \\ e_{31}E_z \\ e_{33}E_z \\ e_{15}E_y \\ e_{15}E_x \\ 0 \end{bmatrix} - \begin{bmatrix} q_{31}H_z \\ q_{31}H_z \\ q_{33}H_z \\ q_{15}H_y \\ q_{15}H_x \\ 0 \end{bmatrix}, \quad (\text{A.1})$$

$$\begin{bmatrix} D_x \\ D_y \\ D_z \end{bmatrix} = \begin{bmatrix} 2e_{31}\varepsilon_{zx} \\ 2e_{31}\varepsilon_{zy} \\ e_{31}\varepsilon_{xx} + e_{31}\varepsilon_{yy} + e_{33}\varepsilon_{zz} \end{bmatrix} + \begin{bmatrix} \kappa_{11}E_x \\ \kappa_{11}E_y \\ \kappa_{33}E_z \end{bmatrix} + \begin{bmatrix} \lambda_{11}H_x \\ \lambda_{11}H_y \\ \lambda_{33}H_z \end{bmatrix}, \quad (\text{A.2})$$

$$\begin{bmatrix} B_x \\ B_y \\ B_z \end{bmatrix} = \begin{bmatrix} 2q_{31}\varepsilon_{zx} \\ 2q_{31}\varepsilon_{zy} \\ q_{31}\varepsilon_{xx} + q_{31}\varepsilon_{yy} + q_{33}\varepsilon_{zz} \end{bmatrix} + \begin{bmatrix} \lambda_{11}E_x \\ \lambda_{11}E_y \\ \lambda_{33}E_z \end{bmatrix} + \begin{bmatrix} \mu_{11}H_x \\ \mu_{11}H_y \\ \mu_{33}H_z \end{bmatrix}. \quad (\text{A.3})$$

Let us consider the displacement, electric and magnetic fields are independent of fiber axis,  $z$ - axis. That is,

$$u_j = u_j(x, y), \quad E_j = E_j(x, y), \quad H_j = H_j(x, y), \quad j = x, y, z. \quad (\text{A.4})$$

We have

$$\varepsilon_{zz} = 0, \quad \varepsilon_{zy} = u_{z,y}, \quad \varepsilon_{zx} = u_{z,x}. \quad (\text{A.5})$$

With the above and the equilibrium equations (3), the problem splits naturally into the two problems

- Plane elasticity and transverse electromagnetic fields

Constitutive laws:

$$\begin{bmatrix} \sigma_{xx} \\ \sigma_{yy} \\ \sigma_{xy} \\ D_z \\ B_z \end{bmatrix} = \begin{bmatrix} C_{11}\varepsilon_{xx} + C_{12}\varepsilon_{yy} \\ C_{12}\varepsilon_{xx} + C_{11}\varepsilon_{yy} \\ 2C_{66}\varepsilon_{xy} \\ e_{31}\varepsilon_{xx} + e_{31}\varepsilon_{yy} \\ q_{31}\varepsilon_{xx} + q_{31}\varepsilon_{yy} \end{bmatrix} + \begin{bmatrix} -e_{31}E_z \\ -e_{31}E_z \\ 0 \\ \kappa_{33}E_z \\ \lambda_{33}E_z \end{bmatrix} + \begin{bmatrix} -q_{31}H_z \\ -q_{31}H_z \\ 0 \\ \lambda_{33}H_z \\ \mu_{33}H_z \end{bmatrix}. \quad (\text{A.6})$$

Equilibrium:

$$\begin{aligned} \sigma_{xx,x} + \sigma_{xy,y} &= 0, \\ \sigma_{xy,x} + \sigma_{yy,y} &= 0. \end{aligned} \quad (\text{A.7})$$

- Anti-plane shear and in-plane electromagnetic fields

Constitutive laws:

$$\begin{bmatrix} \sigma_{zx} \\ \sigma_{zy} \\ D_x \\ D_y \\ B_x \\ B_y \end{bmatrix} = \begin{bmatrix} 2C_{44}\varepsilon_{zx} \\ 2C_{44}\varepsilon_{zy} \\ e_{15}\varepsilon_{zx} \\ e_{15}\varepsilon_{zy} \\ q_{15}\varepsilon_{zx} \\ q_{15}\varepsilon_{zy} \end{bmatrix} + \begin{bmatrix} -e_{15}E_x \\ -e_{15}E_y \\ \kappa_{11}E_x \\ \kappa_{11}E_y \\ \lambda_{11}H_x \\ \lambda_{11}H_y \end{bmatrix} + \begin{bmatrix} -q_{15}H_x \\ -q_{15}H_y \\ \lambda_{11}H_x \\ \lambda_{11}H_y \\ \mu_{11}E_x \\ \mu_{11}E_y \end{bmatrix}. \quad (\text{A.8})$$

Equilibrium:

$$\begin{aligned} \sigma_{zx,x} + \sigma_{zy,y} &= 0, \\ D_{x,x} + D_{y,y} &= 0, \\ B_{x,x} + B_{y,y} &= 0. \end{aligned} \quad (\text{A.9})$$

## References

- [1] L. Rayleigh, *Phil. Mag.* **34**, 481 (1892).
- [2] H.-Y. Kuo, and T. Chen, *Int. J. Eng. Sci.*, **46**, 1157 (2008).
- [3] W. Eerenstein, N. D. Mathur, and J. F. Scott, *Nature* **442**, 759 (2006).
- [4] C.-W. Nan, M. I. Bichurin, S. Dong, D. Viehland, and G. Srinivasan, *J. Appl. Phys.* **103**, 031101 (2008).

- [5] L. D. Landau and E. M. Lifshitz, *Electrodynamics of Continuous Media* (Pergamon Press, New York, 1984) pp.119.
- [6] D. N. Astrov, *Sov. Phys.-JETP* **11**, 708 (1960).
- [7] G. T. Rado and V. J. Folen, *Phys. Rev. Lett.* **7**, 310 (1961).
- [8] C.-W. Nan, *Phys. Rev. B* **50**, 6082 (1994).
- [9] J. H. Huang and W.-S. Kuo, *J. Appl. Phys.* **81**, 1378 (1997).
- [10] Y. Benveniste, *Phy. Rev. B* **51**, 16424 (1995).
- [11] G. Harshé, J. P. Dougherty, and R. E. Newnham, *Int. J. Appl. Electromagn. Mater.* **4**, 161 (1993).
- [12] J. Lee, J. G. Boyd IV, and D. C. Lagoudas, *Int. J. Eng. Sci.*, **43**, 790 (2005).
- [13] J. Y. Li and M. L. Dunn, *Philos. Magazine A* **77**, 1341 (1998).
- [14] J. Y. Li and M. L. Dunn, *J. Intell. Mater. Syst. Struct.* **9**, 404 (1998).
- [15] J. H. Huang, *Phys. Rev. B* **58**, 12 (1998).
- [16] J. Y. Li, *Int. J. Eng. Sci.*, **37**, 5579 (2000).
- [17] T.-W. Wu and J. H. Huang, *Int. J. Solids Struct.* **37**, 2981 (2000).
- [18] H. Huang and L. M. Zhou, *J. Phys. D: Appl. Phys.* **37**, 3361 (2004).
- [19] S. Srinivas, J. Y. Li, A. K. Soh, and Y. C. Zhou, *J. Appl. Phys.* **99** 043905 (2006).
- [20] M. I. Bichurin, V. M. Petrov, and G. Srinivasan, *Phys. Rev. B* **68**, 054402 (2003).
- [21] M. I. Bichurin, V. M. Petrov, O. V. Ryabkov, S. V. Averkin, and G. Srinivasan, *Phys. Rev. B* **72**, 060408 (2005).
- [22] Y. S. Li and P. M. Duxbury, *Phys. Rev. B*, **40**, 4889 (1989).
- [23] O. Fassi-Fehri, A. Hihi, and M. Berveiller, *Int. J. Eng. Sci.* **27**, 495 (1989).
- [24] S.Q. Ren, R.M. Briber, and M. Wuttig, *Appl. Phys. Lett.* **93**, 173507 (2008).
- [25] H.-Y. Kuo and T. Chen, *Int. J. Eng. Sci.*, **45**, 980 (2007).
- [26] V. I. Alshits, A. N. Darinskii, and J. Lothe, *Wave Motion* **16**, 265 (1992).
- [27] J. F. Nye, *Physical Properties of Crystals* (Clarendon Press, Oxford, 1985), pp.300.
- [28] G. B. Arfken and H. J. Weber, *Mathematical Methods for Physicists* (Academic Press, San Diego, 2001).
- [29] C. Kittel, *Introduction to Solid State Physics* (Wiley, New Jersey, 1986), pp.8.

- [30] D. R. Perrins, D. R. McKenzie, and R. C. McPhedran, Proc. Roy. Soc. Lond A **369**, 207 (1979).
- [31] C. L. Berman and L. Greengard, J. Math. Phys. **35**, 6036 (1994).

# The 2009 Joint ASCE-ASME-SES Conference on Mechanics and Materials

## 2009 年 ASCE-ASME-SES 力學與材料聯合會議

服務機關：國立交通大學土木工程學系

姓名職稱：郭心怡 助理教授

前往國家：美國 Blacksburg, Virginia Tech

出國期間：98/06/24~06/27

報告日期：98/07/02



### 一、參加經過

美國工程科學學會 (SES, Society of Engineering Science) 每年固定舉辦力學與材料會議，每四年則與美國土木工程學會 (ASCE, American Society of Civil Engineering)、美國機械工程學會 (ASME, American Society of Mechanical Engineering) 聯合舉行。今年恰逢四年一次的聯合會議，投稿及與會者眾，約六百人次。會議自 6/24 起至 6/27 間於美國 Virginia Tech 舉行，本人的報告於 6/25 第二場次近中午時舉行，雖然美國東岸與台灣時差恰為 12 小時，當時身心還是受時差影響，然報告進行順利，也能理解並回答提問。此次會議為美國本土會議，並無任何參觀觀光行程，純為學術交流與思想激盪。



### 二、心得

美國工程科學學會力學與材料會議雖屬美國本土地區性會議，然由於規模較小，互動較佳，國際間微觀材料力學領域內的頂尖學者皆會與會，例如英國劍橋大學的 Willis 教授、以色列的 de Botten 教授、美國賓州大學的 Ponte Castaneda、美國猶他大學 Chekerv 教授等等。以前在期刊論文上常常看到這些人的文章，能夠親眼見到這些人，聽他們的口頭報告，感覺非常特別。這些人雖已在各自的領域永有一定的聲望，然從其與會時的問答、用餐時的交流，仍能發現其保有研究熱忱與反思能力，並無顯思想上的老態與懶散。期許自己在學術研究上能和他們一樣開創一新的研究方向，並隨著時間的增加仍能具有熱忱與開放的心胸。



### 三、建議

此次會議於 Virginia Tech 舉行，然該校地處偏僻，且校地廣大，無論對外或校內交通皆甚為不便，會議本身雖極具水準，然相關服務支持功能較少，殊為可惜。建議會議主辦單位除考慮會議品質外，應亦花費心思顧慮交通的便捷性。

### 四、攜回資料名稱及內容

1. The 2009 Joint ASCE-ASME-SES Conference on Mechanics and Materials Program  
會議行程
2. 隨身碟：會議文章摘要檔案

# Potential fields of an infinite medium containing arbitrarily positioned elliptic cylinders

Hsin-Yi Kuo\*

Department of Civil Engineering, National Chiao Tung University,  
Hsinchu 30010, Taiwan

The transport phenomena of a heterogeneous medium consisting of multiple cylinders embedded in a host matrix have been a subject of numerous studies. A large number of these studies focused on overall properties of composite materials. In contrast, there have been relatively few studies focused on the details of field solutions. The distributions of the local field are of theoretical and technological values in interpreting various physical phenomena. For instance, it characterizes the extent to which the mutual interactions actually act between the inclusions, and higher-order estimates of the overall properties often require detailed field solutions of the boundary value problem.

The objective of this work is to propose a theoretical framework for evaluation of the potential fields in an unbounded isotropic medium containing a number of elliptic cylinders. We consider the case that the cylinders are arbitrarily positioned subjected to a remotely prescribed potential field. Throughout the formulation, we assume that the cylinders may have different sizes, aspect ratios and with different conductivities. The framework of this study is based on the concept of a multipole expansion formalism, together with a construction of consistency conditions and translation operators. Compared to the integral equations method which often involves a discretization along the interface or over the domain, the interface continuity conditions are directly fulfilled in the formulation, and thus the computation time is greatly reduced. We show that the coefficients of the field expansions are governed by an infinite set of linear algebraic equations. Numerical results are presented for a few different configurations. The derived field solutions can be used to assess the effective conductivity of a random heterogeneous medium.

---

\*E-mail: [hykuo@mail.nctu.edu.tw](mailto:hykuo@mail.nctu.edu.tw)